Int J Adv Manuf Technol (2017) 91:351–361
DOI 10.1007/s00170-016-9735-5

ORIGINAL ARTICLE

Force-based tool condition monitoring for turning process using *v*-support vector regression

Ning Li[1] · **Yongjie Chen**[1] · **Dongdong Kong**[1] · **Shenglin Tan**[1]

Received: 21 June 2016 / Accepted: 7 November 2016 / Published online: 20 November 2016

Abstract In this paper, comprehensive analysis has been carried out to seek out the effective features which can reveal the tool conditions when turning 50# normalized steel. Tool failure mechanism arising in the cutting processes shows that flank wear is the most common failure mode which is taken as the object in this study. Fourteen time-domain features sensitive to tool wear are picked out by utilizing correlation analysis. There are two kinds of tool wear condition, coded as 0 and 1, which is distinguished by the blunt standard. The predictive *v*-support vector regression (*v*-SVR)-based model is constructed to monitor the tool wear conditions. Experimental results show that the prediction accuracy of the *v*-SVR model reaches up to 96.76%. Besides, the *v*-SVR model has better prediction effect and stability than the GRNN- and BPNN-based models.

Keywords Tool condition monitoring · *v*-SVR · Tool failure mechanism · Correlation analysis · Blunt standard

1 Introduction

Progressive wear will appear on the tool rake and flank face in cutting processes. The following situation will happen when tool wear reaches a certain degree, such as significant increase of cutting forces, sharp increment of cutting temperature, chip color changing, and even the occurrence of vibration. Furthermore, severe wear will affect greatly on surface quality of the product, such as machining precision and surface roughness. Worse still, it will lead to the degradation of machining stability. Cutting tools need to be replaced or reground when the tool wear is serious enough to affect the machining efficiency, product quality, and production costs. Therefore, real-time monitoring of the tool wear state is an urgent issue in intelligent manufacturing, which leads to the progress of online tool condition monitoring system, especially in the highly automated production lines.

There are many methods proposed for online tool wear monitoring in the past few decades. However, they are rarely commercialized due to the complexity of the cutting processes, such as nonlinearity and time variation. According to the adopted sensors, these monitoring methods can be divided into direct and indirect methods [1]. The advantage of direct methods, such as machine vision and optical, radioactive, and electrical resistance, is that the actual geometric changes arising from the wear region of the tool can be directly captured. However, direct measurement is very difficult to carry out real-timely owing to the continuous engagement between cutter and workpiece and the disturbance of coolant and chips. These phenomena severely limit the application of direct methods [2]. Recent studies have been mainly focused on the development of indirect methods to monitor the tool wear state. Indirect methods are realized by correlating appropriate sensor signals to tool wear states with the advantages of less complicated setup and greater suitability to practical application [3], such as cutting forces [4–10], vibration [11–15], temperature [16, 17], acoustic emissions [18–22], and spindle current [23]. Remarkably, most of the tool wear monitoring methods were proposed just by utilizing one or two statistic features of a certain domain extracted from force signals, which correlate well with flank wear. And this may not be suitable for other cutting processes owing to the complexity

✉ Dongdong Kong
kodon007@163.com

[1] School of Mechanical Science and Engineering, Huazhong University of Science and Technology, 1037 Luoyu Road, Wuhan, China

and nonuniversality. Besides, many literatures aimed at investigating the effects of a few of discrete tool flank wear values, which could not describe a complete tool wear process [5–7, 12, 15, 19, 20, 23].

Lin et al. [5, 6] measured cutting forces under various cutting parameters in face milling when the flank wear values were set as 0.1, 0.5, and 0.9 mm and established two kinds of tool wear prediction model based on neural network and regression analysis. Axinte et al. [7] attempted to correlate five kinds of specific condition of broaching tools to multiple sensory signals. Chelladurai et al. [12] applied artificial flank wear by EDM to simulate the actual flank wear and developed artificial neural network model based on vibration and strain signals for classification of tool wear. Ku et al. [15] investigated the relationship between three wear states and vibration signal features extracted via wavelet packet based on BP neural network. Li et al. [19] proposed fuzzy clustering method for the recognition of tool wear states using RMS in each frequency band as features based on acoustic emission (AE) signals. Chen et al. [20] performed wavelet multi-resolution analysis on the AE signals during turning free machining mild steel only with a sharp tool and a worn tool. Li et al. [23] also established regression models between cutting parameters and current signals under different tool wear states (0.2, 0.5, and 0.8 mm) and proposed a fuzzy-based classification method to help make the decision about tool replacement. Qiu et al. [24] proposed an approach based on the root mean square of wavelet packet coefficients and hidden Markov model (HMM) for tool wear monitoring.

Among these signals to monitor tool wear and breakage, the cutting forces appear to be more sensitive than others [25]. Indeed, the information carried by force signals has not been fully taken advantage of in most cases. Force signals are highly valid carriers of information about the cutting processes [4]. Therefore, it is of great importance for tool wear monitoring to fully extract the signal features that accurately reflect tool wear degree.

The above literatures show that neural network model is very popular among the researchers attributed to its advantages such as high adaptability and fault tolerance, noise suppression, and data-driven nature [26]. However, its prediction accuracy is limited especially with small sample size resulting from its inherent defects, such as local optimal solution, time-consuming training, overfitting, and poor generalization. Recently, more and more scholars have devoted themselves to the research of support vector machine (SVM). Compared with neural network, SVM has overcome certain shortcomings and shows huge advantage on generalization performance. Shi et al. [8] combined least square support vector machine (LS-SVM) with principal component analysis (PCA) technique to predict tool wear in a broaching operation. Kong et al. [10] presented a new tool wear predictive v-support vector regression (v-SVR)-based model with kernel principal component analysis (KPCA) technique to fuse effective features extracted from force signals. Qian et al. [27] established a SVM with genetic algorithm (SVMG)-based predictive model by learning the relationship between extracted surface texture features and actual tool wear. In addition, there are some varieties of SVM applied to the machining process reported in [28–32].

In the present study, the main objective is to introduce a force-based tool condition monitoring system by utilizing v-SVR [33] and correlation analysis. The correlation coefficient method is applied to select out the effective features while the v-SVR model is trained to identify tool wear states. The experimental results from turning 50# normalized steel show that the v-SVR model has a higher predicted accuracy and a better stability in comparison with generalized regression neural network (GRNN)- [34] and back propagation neural network (BPNN)-based models [6]. The structure of the work is arranged as follows: "Section 2" is a detailed theoretical description about v-SVR. In "Section 3," experimental scheme and tool failure modes are summarized. "Section 4" describes the tool failure mechanism, feature extraction, and construction and validation of v-SVR in detail. In "Section 5," the conclusions are drawn.

2 v-Support vector regression

SVMs are made up of a series of new statistical learning algorithms and especially suitable for the classification and prediction under the condition of small samples. In recent years, the support vector regression (SVR) has been developed to approximate nonlinear functions by arbitrary accuracy with a global minimum and a fast convergence speed. In the ε-SVR algorithm, the argument ε will contribute to achieving the desired approximation accuracy which is specified in advance. In order to make the parameter selection more easy, an improved version ν-SVR was put forward by Schölkopf [33]. The number of boundary support vectors and support vectors can be controlled by selecting a suitable parameter ν. The principle of ν-SVR algorithm is presented as below.

Given a training set $\{\boldsymbol{x}_i, y_i\}_{i=1}^{N}$, $\boldsymbol{x}_i \in \boldsymbol{R}^n$, $y_i \in \boldsymbol{R}$, the regression problem needs to solve a mapping function $f: \boldsymbol{R}^n \rightarrow \boldsymbol{R}$, from the input space to the output space, which makes $f(\boldsymbol{x}) = y$. While the objective of ν-SVR algorithm is to seek to estimate functions,

$$y = f(\boldsymbol{x}) = (\boldsymbol{w} \cdot \boldsymbol{x}) + b \tag{1}$$

where $\boldsymbol{w}, \boldsymbol{x} \in \boldsymbol{R}^n, b \in \boldsymbol{R}$. At every point $\boldsymbol{x_i}$, an error of ε is permitted. The one beyond this error is compromised by slack variables ξ_i and ξ_i^* and punished through a regularization constant C in the objective function. The value of ε is weighed against the complexity of the model and slack variables through a constant $v \geq 0$. According to the statistical learning

theory, ν-SVR algorithm is designed based on structural risk minimization to obtain the regression function for the linear problem, namely solving the minimum value of the following cost function:

$$\tau\left(\boldsymbol{w},\xi,\xi^{*},\varepsilon\right)=\frac{1}{2}\|\boldsymbol{w}\|^{2}+C\cdot\left(\nu\varepsilon+\frac{1}{N}\sum_{i=1}^{N}\left(\xi_{i}+\xi_{i}^{*}\right)\right) \quad (2)$$

subject to:

$$((\boldsymbol{w}\cdot\boldsymbol{x}_{i})+b)-y_{i}\leq\varepsilon+\xi_{i} \quad (3)$$

$$y_{i}-((\boldsymbol{w}\cdot\boldsymbol{x}_{i})+b)\leq\varepsilon+\xi_{i}^{*} \quad (4)$$

$$\varepsilon\geq0,\xi_{i}\geq0,\xi_{i}^{*}\geq0 \quad (5)$$

where $\|\boldsymbol{w}\|^{2}$ stands for the complexity of the model, ε denotes insensitive training errors, C is a constant which determines the weight value between the complexity of the model and the training errors, and v is a new introduced parameter.

To solve this optimization problem, Lagrange multiplier techniques are used to construct the Lagrange function as

$$\begin{aligned}&L\left(w,b,\alpha,\alpha^{*},\beta,\xi,\xi^{*},\varepsilon,\eta,\eta^{*}\right)\\&=\tau\left(w,\xi,\xi^{*},\varepsilon\right)-\beta\varepsilon-\sum_{i=1}^{N}\left(\eta_{i}\xi_{i}+\eta_{i}^{*}\xi_{i}^{*}\right)-\sum_{i=1}^{N}\alpha_{i}(\xi_{i}+y_{i}-(w\cdot x_{i})-b+\varepsilon)\\&-\sum_{i=1}^{N}\alpha_{i}^{*}(\xi_{i}^{*}+(w\cdot x_{i})+b-y_{i}+\varepsilon)\end{aligned} \quad (6)$$

where $\alpha_{i},\alpha_{i}^{*},\eta_{i},\eta_{i}^{*},\beta\geq0$ are Lagrange multipliers. The solution of Eq. (6) can be obtained by finding the saddle point of L. Setting the partial derivatives of function L with respect to the primal variables $\boldsymbol{w},b,\xi_{i},\xi_{i}^{*},\varepsilon$ to zero yields the following equations:

$$\begin{cases}w=\sum_{i}\left(\alpha_{i}^{*}-\alpha_{i}\right)x_{i}\\\sum_{i=1}^{N}\left(\alpha_{i}-\alpha_{i}^{*}\right)=0\\\frac{C}{N}-\alpha_{i}-\eta_{i}=0\\\frac{C}{N}-\alpha_{i}^{*}-\eta_{i}^{*}=0\\C\cdot\nu-\sum_{i}\left(\alpha_{i}+\alpha_{i}^{*}\right)-\beta=0\end{cases} \quad (7)$$

Finally, the resulting regression estimate can be obtained as follows after solving the above equations:

$$f(x)=\sum_{i=1}^{N}\left(\alpha_{i}^{*}-\alpha_{i}\right)(x_{i},x)+b \quad (8)$$

The above regression estimate is linear, not suitable for the nonlinear cutting process, especially for tool condition monitoring. However, this algorithm can be extended to a nonlinear one by adopting the kernel function method, namely, replacing the dot product with a kernel function K which does the dot product in feature space related to input space through a nonlinear mapping Φ. In this research, RBF kernel is selected as the kernel function as the following:

$$K\left(x_{i},x_{j}\right)=\left(\Phi(x_{i})\cdot\Phi\left(x_{j}\right)\right)=\exp\left(-\left\|x_{i}-x_{j}\right\|^{2}\Big/\left(2\sigma^{2}\right)\right) \quad (9)$$

Then, the regression estimate for nonlinear problem can be expressed as

$$f(x)=\sum_{i=1}^{N}\left(\alpha_{i}^{*}-\alpha_{i}\right)K(x_{i},x)+b \quad (10)$$

In the Eq. (10), only the nonzero α_{i}^{*} and α_{i} will precisely meet the constraints of Eq. (3) or (4). The corresponding patterns are referred to as support vectors which completely determine the regression function $f(\boldsymbol{x})$.

3 Experimental setup

Before the v-SVR-based predictive model is constructed, the relationship between signal features and tool wear degree needs to be confirmed. The effective features are extracted from force signals collected from cutting tests.

3.1 Experimental components

The workpieces utilized in this study are round bars with the dimension of 200-mm diameter and 500-mm length, which were made of 50# normalized steel (HB160~197). The cutting tests are performed on a DMTG-CW6163E turning lathe. The experimental components are listed in Table 1. The diagram of experimental platform for cutting force acquisition and tool wear measurement is illustrated in Fig. 1. The dynamometer is mounted under the tool rest with eight bolts. The image measuring system VMS-1510G is used to observe the tool flank wear.

Table 1 Experimental components

Components	Type
Engine lathe	DMTG-CW6163E
Indexable inserts	Sandvik CNMG120408-PM
Tool holder	Sandvik PCLNR 2525M 12
Dynamometer	Kistler 9257A
Charge amplifier	Kistler 5070A
Data acquisition system	Kistler 5697A
Notebook with DynoWare	Kistler 2825A
Video measuring system	VMS-1510G (QIM1008)

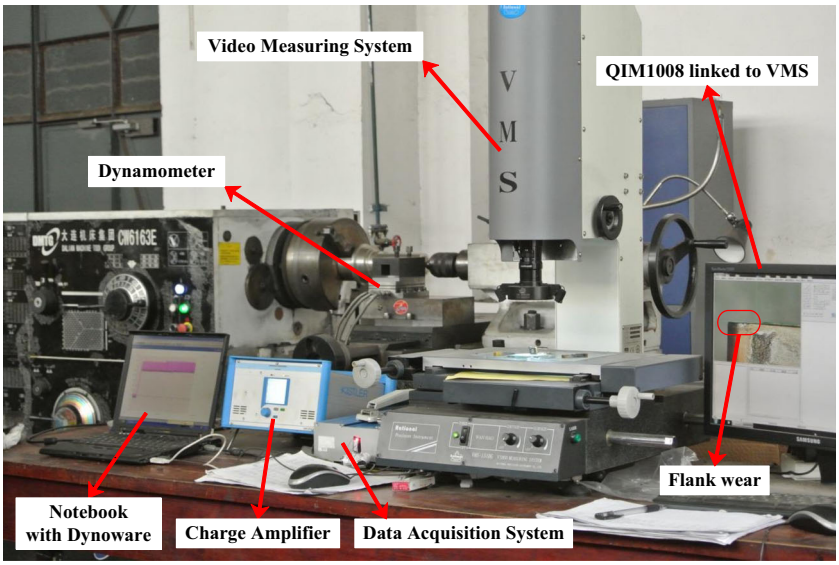

Fig. 1 The diagram of experimental platform for cutting force acquisition and tool wear measurement

3.2 Design of experiments

The objectives of this study are to analyze the cutting force signals and to extract the effective features that correlate well with tool wear from the signals obtained during turning of 50# normalized steel. In order to ensure tool wear as normal as possible, trial cuts are quite necessary to confirm the range of cutting parameters so as to reduce chatter or vibration and verify the feasibility of the selected parameters.

The selected nine sets of cutting parameters are list in Table 2. Three cutting tests are carried out for each set of cutting parameters since there are various tool wear types happening during the tests and the occurrence appears to be highly random, even for the same cutting parameters [35]. All these tests are performed in dry condition to acquire cutting force signal sampling at 20 kHz. Each insert will undergo the process from fresh tool to worn-out under each set of cutting parameters as shown in Table 2. The blunt standard will be introduced in the next section. Besides, flank wear of the insert is measured by utilizing VMS-1510G at 2-min intervals or longer so that the tool wear state in each stage is recorded. The cutting process will not be terminated until the insert is severely worn.

4 Results and discussions

4.1 Tool failure mechanism

Apart from normal wear like flank wear, crater wear, and notch wear, there are several other failure modes, such as built-up edge, chipping, tipping, and hot crack, on the tools engaged in the machining process as shown in Table 2. It can be observed that flank wear is the most common failure mode and appears in the whole life and under all conditions. The other failure modes could suddenly emerge after the flank wear increased to a certain extent which means the inserts

Table 2 Experimental cutting parameters and the corresponding failure mode

Test no.	Cutting speed V_c (m/min)	Cutting depth a_p (mm)	Feed rate f (mm/r)	Tool main failure mode
1~3	300	1	0.3	Flank wear, crater wear, tipping
4~6	300	2	0.3	Flank wear, hot crack, chipping
7~9	350	1	0.3	Flank wear, built-up edge, tipping
10~12	300	1	0.2	Flank wear, crater wear
13~15	300	1	0.4	Flank wear, built-up edge, tipping
16~18	300	2	0.4	Flank wear, hot crack, chipping, crater wear
19~21	350	1	0.4	Flank wear, built-up edge, tipping
22~24	300	2	0.2	Flank wear, hot crack, chipping
25~27	350	1	0.2	Flank wear, tipping, crater wear

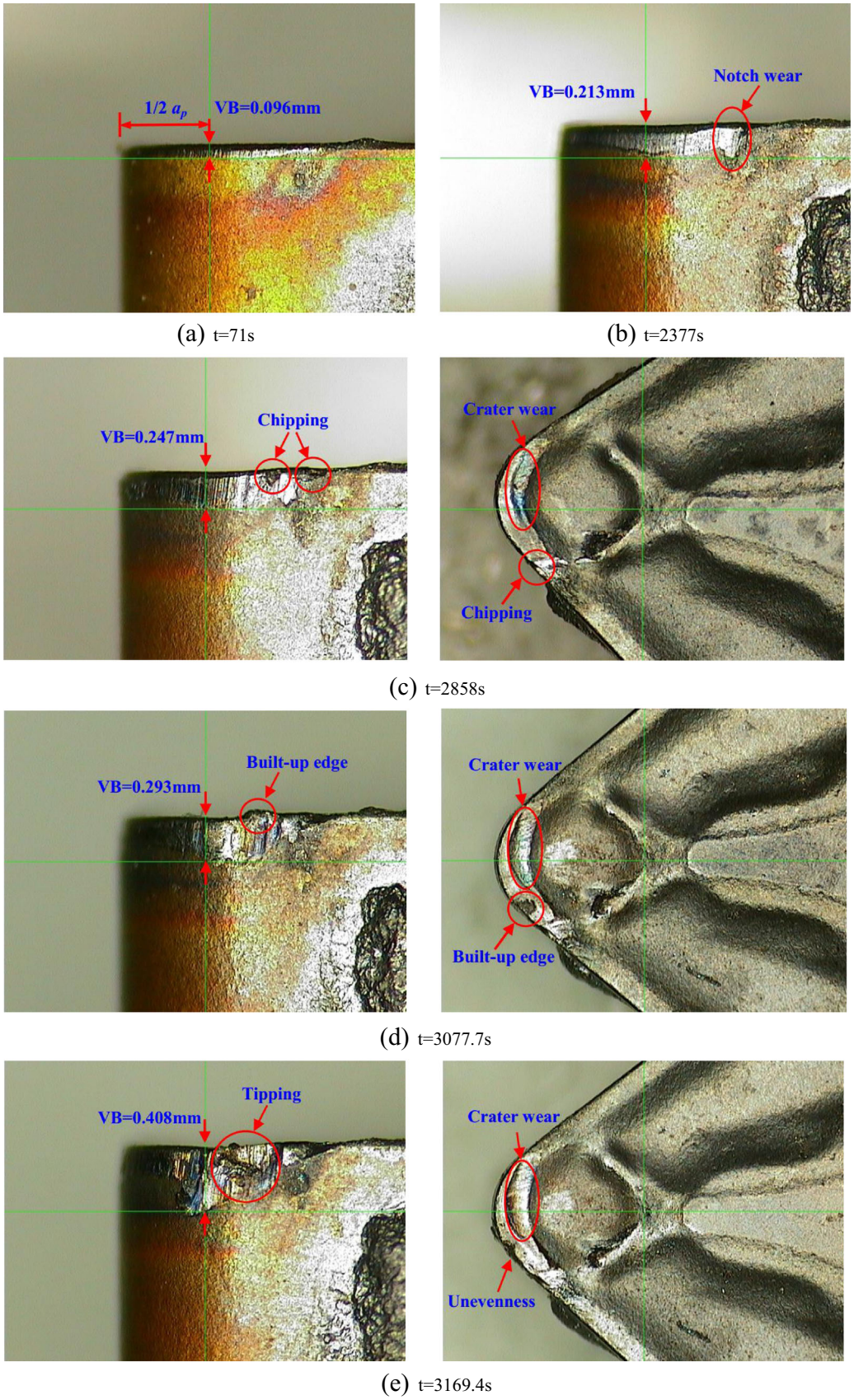

Fig. 2 Failure modes of the insert (Test no. 25) with the cutting time of: (**a**) 71s, (**b**) 2377s, (**c**) 2858s, (**d**) 3077.7s and (**e**) 3169.4s

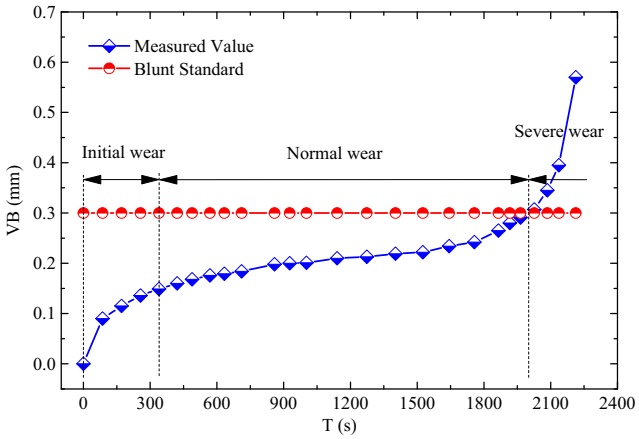

Fig. 3 The variation of flank wear VB with the cutting time (Test no. 23)

are on the verge of broken. It also indicates that hot crack mainly appears in the case of large cutting depth, caused by uneven distribution of cutting heat. Surface topography of the failure modes happened in the inserts is illustrated in Fig. 2 after the machining tests of 50# normalized steel in Test no. 25. In this figure, VB refers to tool flank wear land width, a variable quantifying flank wear. It can be seen that only flank wear was clearly observed in the beginning due to attrition caused by mechanical stress as shown in Fig. 2a. With the increasing of flank wear as shown in Fig. 2b, notch wear becomes more obvious mainly due to the constant friction and impact between cutting edge and hardened layer of the workpiece surface. In addition, crater wear has not been observed. The cutting edge where notch wear repeated occurrence started to chip and a few small gaps were formed as shown in Fig. 2c. The constant impact of the workpiece surface hardened layer on the cutting edge leads to the appearance of fatigue fracture. Meanwhile, the rudiment of crater wear on rake face could be discovered, mainly caused by high temperature, high pressure, and severe friction in the tool-chip interface. As time went by, built-up edge was detected on the rake face near the tool major cutting edge as shown in Fig. 2d. It is likely because cold welding of the chip happens on the rake face under the conditions of proper temperature and high pressure. At this moment, flank wear and crater wear have become worse. Figure 2e indicates that the insert is seriously worn accompanied by the phenomenon of tipping near the cutting edge on flank face. The tipping on the flank face leads to uneven fragile edge, caused by severe vibration. This marks the end of the tool life. It can be concluded from Fig. 2 that flank wear plays an important role in the whole tool life, which tends to be accompanied by other failure modes.

4.2 Tool flank wear

It is well known that the tool needs to be replaced when tool wear reaches a certain degree, i.e., blunt standard. In general, flank wear has a more significant effect on surface quality, cutting force, and cutting temperature than rake wear. It appears in the whole tool life under all conditions and is easier to be measured than other types of wear during the gradual wear process. The blunt standard is laid down based on the tool flank wear land width. In this work, the wear value VB at the location of 1/2 a_p on the flank face was taken as an object of study [36].

The flank wear increased with the cutting time went on as illustrated in Fig. 3. Its trend was consistent with the pattern reported by other researchers [36, 37]. VB denotes the tool flank wear land width measured after each cutting process. The blunt standard is set as 0.3 mm, meaning the tool is worn out or breakage and should be replaced when VB exceeds this threshold value. It can be observed that the inserts went through three stages in its life, namely initial wear, normal wear, and severe wear. Usually, the blunt standard is used to distinguish normal wear from severe wear. However, there is no clear boundary between initial wear and normal wear. Besides, the initial wear is transient. Therefore, initial wear is classified as normal wear in this work. The symbolic state is severe wear, which manifests the tool should be replaced and has an important significance in the field of mechanical manufacturing.

4.3 Feature extraction and selection

The number of the selected features should be as large as possible so that the wear state can be exactly described. Most of the features extracted from force signals are subject to the cutting conditions, so they could not be selected to predict the current state of tool wear under different cutting conditions [35]. Besides, tool wear has a great relevance with cutting parameters which are not dependent on the extracted features and chosen as the features to describe tool wear states [19]. Therefore, it is hoped that the selected features should not be too sensitive to cutting conditions and these features should have a strong correlation with tool wear in any cutting

Table 3 The average correlation coefficients (CCs) between VB and extracted features

Features	Mean_F_x	Mean_F_y	Mean_F_z	Max_F_x	Max_F_y	Max_F_z	Resultant force
CCs	0.93	0.93	0.88	0.89	0.83	0.71	0.92
Features	Rms_F_x	Rms_F_y	Rms_F_z	F_x/F_z	F_y/F_z	Power	Moment of F_x
CCs	0.93	0.92	0.88	0.92	0.90	0.88	0.91

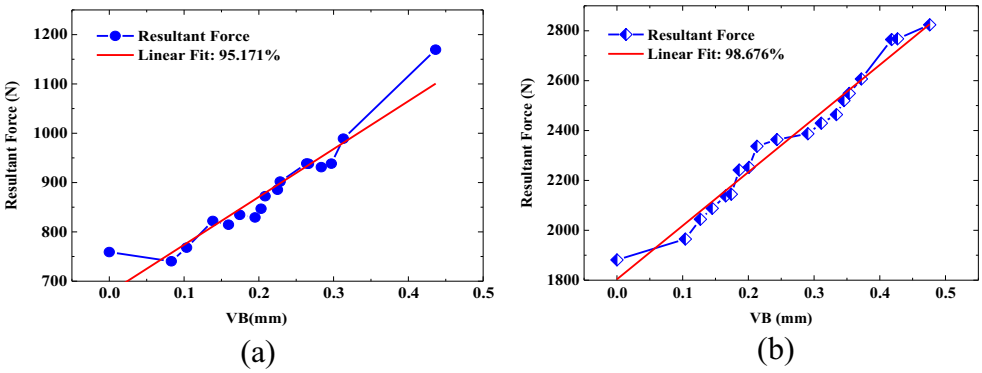

Fig. 4 Resultant force vs. VB for (**a**) Test No. 8 and (**b**) Test No. 17

conditions. Thus, this tool wear monitoring system can be suitable for various cutting conditions.

In order to remove the redundant features which have little relevance to tool wear, correlation analysis is introduced as a feature filter to weigh up this relevance criterion for feature selection. Correlation analysis is always utilized to describe the linear correlation between two signals. The correlation coefficient is expressed as

$$\rho_{xy} = \frac{\sum_{i=1}^{n}\left(x_i-\bar{x}\right)\left(y_i-\bar{y}\right)}{\sqrt{\sum_{i=1}^{n}\left(x_i-\bar{x}\right)^2\left(y_i-\bar{y}\right)^2}} \tag{11}$$

where x_i stands for the preliminary extracted feature, while y_i stands for the corresponding tool wear value. $\bar{x}$ and $\bar{y}$ are the mean values, respectively. Correlation coefficient changes between −1 and 1. The more the absolute value $|\rho_{xy}|$ is close to 1, the better the linear correlation between the feature and tool wear is conformed. It means this feature is sensitive to tool wear and can be used to describe the characteristic of tool wear.

When the absolute values of correlation coefficient between extracted features and tool wear are greater than or equal to 0.6 in all cutting conditions, the features are selected. The discriminant features are extracted from force signals by time-domain statistical analysis. And the calculation of correlation coefficient between these features and VB is also carried out. The selected effective features after taking the average of the correlation coefficients are presented in Table 3. These 14 features are utilized to describe the current tool wear states real-timely.

Resultant force and moment of F_x versus average flank wear (VB) under different cutting parameters are illustrated in Figs. 4 and 5, respectively. A good correlation can be observed between the features and VB which indicates these features can be used to predict tool wear.

While most of the other features may have a consistent correlation with VB in certain cutting conditions such as crest factors, they appear to fluctuate once the condition is changed, showing weaker associations with flank wear. Figure 6 illustrates the relationship between the crest factors (Cre_F_x, Cre_F_y) and flank wear under different cutting conditions. It can be found that the crest factors have a good correlation with VB in Fig. 6a, while they are irregular in Fig. 6b. Therefore, these features should not be selected.

Before constructing the v-SVR model, all the selected features should be normalized through zero-mean normalization method with the formula as following,

$$x' = \frac{x-\mu}{\sigma} \tag{12}$$

where μ and σ stand for mean and standard deviation, respectively. The 14 normalized features as shown in Table 3 and three cutting parameters will be taken as the input of the v-SVR model as presented in "Section 2."

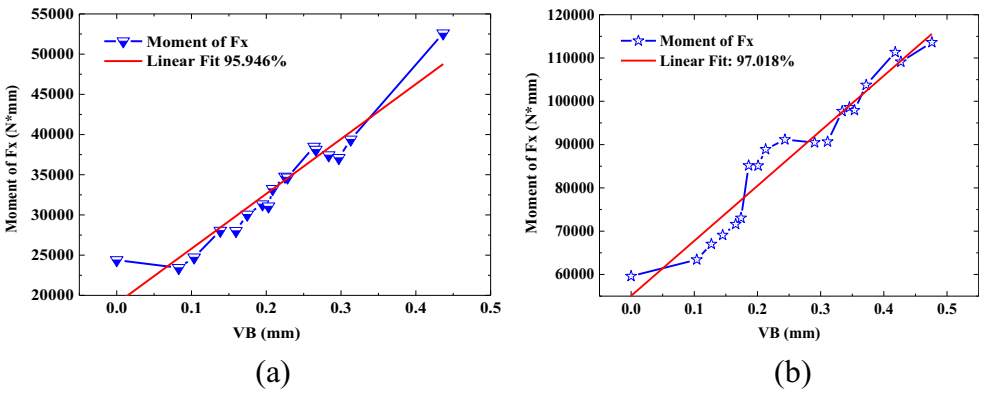

Fig. 5 Moment of F_x vs. VB for (**a**) Test No. 8 and (**b**) Test No. 17

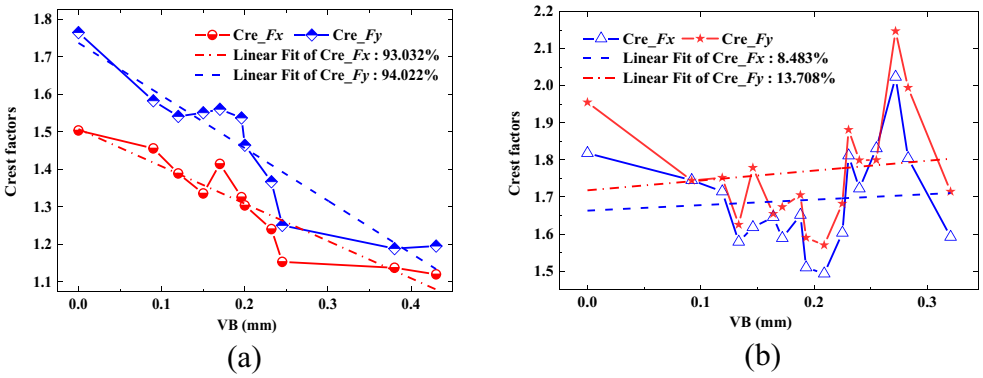

Fig. 6 Crest factors vs. VB for (**a**) Test No. 6 and (**b**) Test No. 20

4.4 Experimental results and discussion

Before building the ν-SVR model, normalization processing for the above features is helpful for argument selection and improvement of training speed. There are two important arguments: gamma ($-g$) and cost ($-c$) needed to be determined during the training process. In general, the grid-search and the cross-validation methods are utilized together to achieve the best g and the best c during which a good accuracy is obtained. In this way, the ν-SVR model is constructed. The tool wear state can be classified into two types in this paper, namely normal wear and severe wear [19]. Two wear states based on the flank wear value are listed in Table 4.

There are a total of 463 cutting processes during the 27 groups of cutting tests. One signal containing cutting forces in three dimensions (X, Y, and Z) is obtained from each cutting process. Two sets of the selected features are randomly extracted from each signal, one for training and the other for testing. Testing samples will not appear in the training samples. The corresponding label for each set of features is created according to the classification in Table 4. Then, the model based on ν-SVR for tool wear prediction will be trained by using training samples and the corresponding labels. Combining grid-search with cross-validation method, the best arguments g and c are obtained as 0.0313 and 512, respectively. The parameters b, α_i^*, and α_i in "Section 2" are also worked out, and the tool wear model is well constructed. Testing data are utilized to verify the prediction accuracy of this ν-SVR-based tool wear model. The predicted results and the actual tool states are presented in Fig. 7. The results show that the average accuracy of this model reaches up to 96.76%. Once the predicted label is "1," it represents the tool is severely worn and should be replaced in time.

Table 4 Tool wear state classification

Tool states	Tool flank wear land width	Labels
Normal wear	0 < VB < 0.3 mm	0
Severe wear	VB > 0.3 mm	1

At the same time, the tool wear models based on GRNN and BPNN are also trained and tested by the same data sets, respectively. The classification results are presented in Figs. 8 and 9, respectively. The scattered points in these two figures indicate that the prediction accuracy is not satisfactory, especially in the BPNN model. The results predicted by GRNN and BPNN models have a great uncertainty because of the initial weights and thresholds randomly generated in the training process.

Classification rate of ν-SVR, GRNN, and BPNN for the 27 groups of cutting tests under nine sets of cutting parameters is listed in Table 5. Each set of cutting parameters is repeated three times. Classification results reveal that the accuracy and stability of ν-SVR are superior to GRNN and BPNN. Besides, the robustness and reproducibility of ν-SVR make it more reliable for tool wear monitoring in industrial environments.

4.5 Superiority of ν-SVR in small samples

In order to investigate the generalization ability of the models, different sizes of samples are applied to train these three models. Taking one set of cutting parameters as an example, comparison of the predicted accuracy by three models under the same testing samples is carried out as shown in Fig. 10. The numbers 1/3, 1/2, and 1/1 in the figure represent the ratios of size between testing samples and training samples.

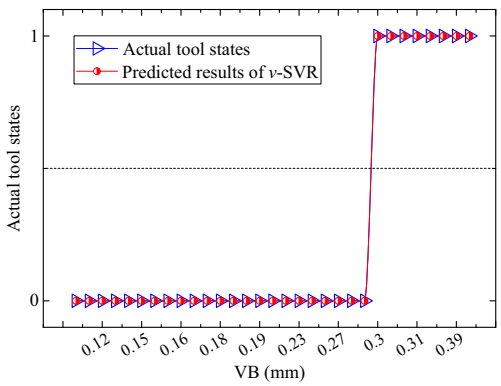

Fig. 7 The predicted results of ν-SVR model and the actual tool states (Test no. 10)

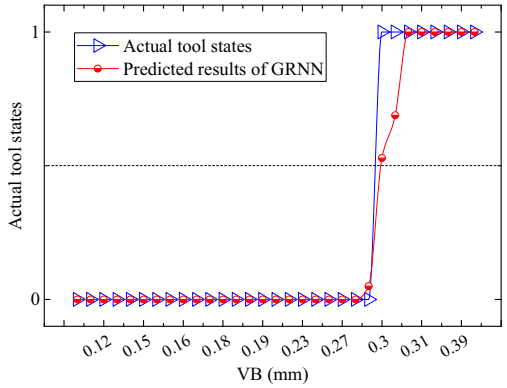

Fig. 8 The predicted results of GRNN and the actual tool states (Test no. 10)

Contents in brackets stand for the training sample size. The predicted accuracy of the *v*-SVR model is almost the same with the sharp reduction of training sample size. The accuracy of the GRNN model has a certain decrease as training sample size decreases and is lower than that of *v*-SVR model. However, the accuracy of the BPNN model shows a sharp decline with the decrease of training sample size. The above analysis reveals that *v*-SVR model has better generalization ability even under the condition of small sample. The comparison result also shows that the tool wear model based on *v*-SVR can keep a high success rate to predict tool wear even when the training sample size is sharply reduced. Besides, the average time of training and testing for *v*-SVR, GRNN, and BPNN is 1.096, 80.686, and 2.25 s, respectively. Therefore, *v*-SVR shows great superiority over GRNN and BPNN in the aspect of small sample size and training speed.

Table 5 Classification rate of *v*-SVR, GRNN, and BPNN (%)

Test no.	V_c (m/min)	a_p (mm)	f (mm/r)	*v*-SVR	GRNN	BPNN
1	300	1	0.3	93.75	75	81.25
2	300	1	0.3	95.24	61.9	61.9
3	300	1	0.3	95.24	66.67	90.48
4	300	2	0.3	93.33	93.33	60
5	300	2	0.3	100	100	75
6	300	2	0.3	100	100	81.82
7	350	1	0.3	84.62	61.54	61.54
8	350	1	0.3	94.12	64.71	82.35
9	350	1	0.3	92.31	76.92	76.92
10	300	1	0.2	100	90.32	70.97
11	300	1	0.2	96.77	90.32	87.1
12	300	1	0.2	100	93.33	93.33
13	300	1	0.4	100	100	92.86
14	300	1	0.4	100	80.95	95.24
15	300	1	0.4	93.33	86.67	100
16	300	2	0.4	100	70	40
17	300	2	0.4	94.74	73.68	52.63
18	300	2	0.4	100	100	70
19	350	1	0.4	88.89	33.33	44.44
20	350	1	0.4	100	52.94	64.71
21	350	1	0.4	84.62	76.92	84.62
22	300	2	0.2	100	96	84
23	300	2	0.2	100	92	76
24	300	2	0.2	100	100	60
25	350	1	0.2	100	100	95.83
26	350	1	0.2	100	92.86	92.86
27	350	1	0.2	92.31	84.62	84.62
Average				96.76	83.15	77.97

5 Conclusions

It is well known that one of the most critical issues for monitoring tool wear is to select the features extracted from the original signals which can accurately describe the tool wear state. In this work, a new method based on *v*-SVR is introduced to monitor the tool condition in turning operations. The 14 selected features derived from time-domain statistical analysis show a good correlation with tool flank wear. This paper provides a more reliable solution for tool wear state estimation under industrial circumstance.

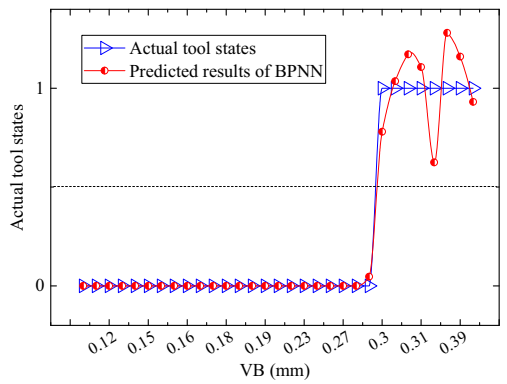

Fig. 9 The predicted results of BPNN and the actual tool states (Test no. 10)

This study concludes as following:

1. There are several tool failure modes engaged in the machining process, including flank wear, crater wear and notch wear, built-up edge, chipping, tipping, and hot crack. Thereinto, flank wear is the most common failure mode and appears in the whole tool life.
2. Correlation analysis reveals that not all the features are suitable for tool wear monitoring. Only the features that correlate well with tool wear in different cutting conditions are considered to be effective. The selected features have higher average correlation coefficient which is more than 0.6.
3. The inserts go through three stages in its life, namely initial wear, normal wear, and severe wear. In this work,

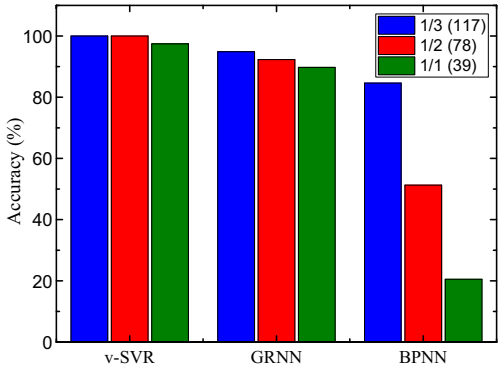

Fig. 10 Comparison of the predicted accuracy by three models (Test nos. 16, 17, and 18)

initial wear is classified as normal wear. The blunt standard set at 0.3 mm is utilized to distinguish normal wear and severe wear.

4. The *v*-SVR-based method is successfully incorporated into monitoring of tool wear state. Compared with GRNN and BPNN models, the *v*-SVR model has a higher predicted accuracy reaching up to 96.76%. Besides, the *v*-SVR model shows great superiority over GRNN and BPNN models in stability, robustness, repeatability, small sample size, and training speed.

Acknowledgments The authors are grateful to the financial sponsorship from the National Science and Technology Major Project of China (Grant no. 2012ZX04003-021). Besides, the authors are grateful to all the partners for their valuable contributions to this work.

References

1. Li D, Mathew J (1990) Tool wear and failure monitoring techniques for turning—a review. Int J Mach Tools Manuf 30(4):579–598
2. Sick B (2002) On-line and indirect tool wear monitoring in turning with artificial neural networks: a review of more than a decade of research. Mech Syst Signal Process 16(4):487–546
3. Ghani JA, Rizal M, Nuawi MZ, Ghazali MJ, Haron CHC (2011) Monitoring online cutting tool wear using low-cost technique and user-friendly GUI. Wear 271:2619–2624
4. Oraby SE (1995) Monitoring of turning operation via force signals part 1: recognition of different tool failure forms by spectral analysis. Wear 184:133–143
5. Lin SC, Ting CJ (1995) Tool wear monitoring in drilling using force signals. Wear 180:53–60
6. Lin SC, Lin RJ (1996) Tool wear monitoring in face milling using force signals. Wear 198:136–142
7. Axinte DA, Gindy N (2003) Tool condition monitoring in broaching. Wear 254:370–382
8. Shi DF, Gindy NN (2007) Tool wear predictive model based on least squares support vector machines. Mech Syst Signal Process 21(4):1799–1814
9. Fang N, Pai P, Mosquea S (2011) Effect of tool edge wear on the cutting forces and vibrations in high-speed finish machining of inconel 718: an experimental study and wavelet transform analysis. Int J Adv Manuf Technol 52:65–77
10. Kong DD, Chen YJ, Li N, Tan SL (2016) Tool wear monitoring based on kernel principal component analysis and v-support vector regression. Int J Adv Manuf Technol. doi:10.1007/s00170-016-9070-x
11. Dimla SDE (2002) The correlation of vibration signal features to cutting tool wear in a metal turning operation. Int J Adv Manuf Technol 19:705–713
12. Chelladurai H, Jain V, Vyas N (2008) Development of a cutting tool condition monitoring system for high speed turning operation by vibration and strain analysis. Int J Adv Manuf Technol 37:471–485
13. Prasad B, Sarcar M, Ben B (2010) Development of a system for monitoring tool condition using acousto-optic emission signal in face turning—an experimental approach. Int J Adv Manuf Technol 51:57–67
14. Ding F, He Z (2011) Cutting tool wear monitoring for reliability analysis using proportional hazards model. Int J Adv Manuf Technol 57:565–574
15. Ku XC, Zhou YM, Gao PL, Duan MD (2014) Recognition of tool wear state based on wavelet packet and BP neural network. Modern Manufacturing Engineering 12:68–72
16. Choudhury SK, Bartarya G (2003) Role of temperature and surface finish in predicting tool wear using neural network and design of experiments. Int J Mach Tools Manuf 43(7):747–753
17. Singh D, Rao PV (2010) Flank wear prediction of ceramic tools in hard turning. Int J Adv Manuf Technol 50:479–493
18. Ravindra HV, Srinivasa YG, Krishnamurthy R (1997) Acoustic emission for tool condition monitoring in metal cutting. Wear 212(1):78–84
19. Li XL, Yuan ZJ (1998) Tool wear monitoring with wavelet packet transform—fuzzy clustering method. Wear 219(2):145–154
20. Chen XZ, Li BZ (2007) Acoustic emission method for tool condition monitoring based on wavelet analysis. Int J Adv Manuf Technol 33:968–976
21. Bhuiyan M, Choudhury I, Yusoff N (2012) A new approach to investigate tool condition using dummy tool holder and sensor set-up. Int J Adv Manuf Technol 61:465–479
22. Jemielniak K, Urbański T, Kossakowska J, Bombiński S (2012) Tool condition monitoring based on numerous signal features. Int J Adv Manuf Technol 59:73–81
23. Li XL, Tso SK (1999) Drill wear monitoring based on current signals. Wear 231(2):172–178
24. Qiu Y, Xie FY (2014) Tool wear monitoring based on wavelet packet coefficient and hidden Markov model. Hydromechatronics Engineering 42(12):40–44
25. Li GS, Lau WS, Zhang YZ (1992) In-process drill wear and breakage monitoring for a machining center based on cutting force parameters. Int J Mach Tools Manuf 32(6):855–867
26. Siddhpura A, Paurobally R (2013) A review of flank wear prediction methods for tool condition monitoring in a turning process. Int J Adv Manuf Technol 65:371–393
27. Qian YQ, Tian J, Liu LB, Zhang Y, Chen YS (2010) A tool wear predictive model based on SVM. In: 2010 Chinese control and decision conference, pp 1213–1217
28. Wang LW, Wang J (2012) Cloud-SVM model and its application in the prediction of CNC machine tool wear state. Modular Machine Tool & Automatic Manufacturing Technique 09:25–31
29. Nie P, Dong H, Li ZQ, Gao H, Li B (2013) State recognition of tool wear based on improved empirical mode decomposition and least squares support vector machine. Journal of Beijing University of technology 39(12):1784–1790
30. Peng MW, Chen HT, Zhong CM (2014) Decision fusion techniques of tool wear state based on SVM. Modular Machine Tool & Automatic Manufacturing Technique 04:89–93
31. Li SC, Li W, Wu MM (2015) Study on the application of feature fusion and GA-SVM in cutting tool wear monitoring. Manufacturing Technology & Machine Tool 04:145–148

32. Li WL, Fu P, Cao WQ (2015) Study on the technology of tool wear monitoring by modifying least square support vector machine via Kalman filter. Mechanical Science and Technology for Aerospace Engineering 34(1):81–85
33. Sch lkopf B, Smola AJ, Williamson RC, Bartlett PL (2000) New support vector algorithms. Neural Comput 12(5):1207–1245
34. Specht DF (1991) A general regression neural network. IEEE Transactions on Neural Networks 2(6):568–576
35. Nouri M, Fussell BK, Ziniti BL, Linder E (2015) Real-time tool wear monitoring in milling using a cutting condition independent method. Int J Mach Tools Manuf 89:1–13
36. Chen RY (2002) Metal cutting principles. China Machine Press, Beijing
37. Xiong LS, Yan XG, Zhang FR (2006) Fundamentals of mechanical manufacturing technology. Huazhong University of Science and Technology Press, Wuhan